Comparative Biochemistry and Physiology, Part D 5 (2010) 171–177

Contents lists available at ScienceDirect

Comparative Biochemistry and Physiology, Part D

journal homepage: www.elsevier.com/locate/cbpd

Multi-transcript expression patterns in the gastrolith disk and the hypodermis of the crayfish *Cherax quadricarinatus* at premolt

Yana Yudkovski [a,1], Lilah Glazer [b,c,1], Assaf Shechter [b,c], Richard Reinhardt [d], Vered Chalifa-Caspi [c], Amir Sagi [b,c], Moshe Tom [a,*]

[a] Israel Oceanographic and Limnological Research, P.O.B 8030, Haifa 31080, Israel
[b] Department of Life Sciences, Ben-Gurion University of the Negev, Beer-Sheva 84105, Israel
[c] The National Institute for Biotechnology in the Negev, Ben-Gurion University of the Negev, Beer-Sheva 84105, Israel
[d] Max Plank Institute-Molecular Genetics, Ihnestrasse 63, D-14195 Berlin-Dahlem, Germany

ARTICLE INFO

Article history:
Received 9 December 2009
Received in revised form 30 March 2010
Accepted 30 March 2010
Available online 7 April 2010

Keywords:
Arthropods
Crustaceans
Molt cycle
Gastrolith disk
Hypodermis
Chitin deacetylase

ABSTRACT

In the crustacean *Cherax quadricarinatus*, alterations of multi-transcript expression patterns between intermolt and late premolt stages were identified in the hypodermis and in the gastrolith disk via a cDNA microarray. The gastrolith disk is a specialized epithelium forming the gastroliths at premolt. The gastroliths are deposits of calcium carbonate derived from the digested cuticle contributing the mineral to the newly formed exoskeleton at postmolt. The late premolt stage was characterized by a dramatic general up-regulation of genes in the gastrolith disk. This phenomenon is explained by the gastrolith disk function rapid formation of the relatively large gastrolith during a short period of time. Besides genes of general importance for this dramatic change, three genes related to the chitin–protein–mineral structure were identified. The cDNA and the deduced protein of the novel one of them, the chitin deacetylase 1 (Cq-CDA1) was fully characterized and its resemblance to already characterized structural proteins of the gastrolith matrix was described. Cq-CDA1 characteristics strongly indicate its participation in the gastrolith construction, although its protein product was not identified yet in the gastrolith. In addition, many differentially expressed genes with unknown function were elucidated. An unexpected milder down-regulation was observed in the hypodermis.

1. Introduction

Similar to all arthropods, crustacean growth and development is a stepwise process involving the periodic shedding and subsequent reconstruction of a rigid external exoskeleton — the cuticle. The compounds responsible for the partial degradation of the old cuticle and the construction of the new one are synthesized in, or transported through the underlying hypodermis, which is composed mainly of a layer of epithelial cells, accompanied by other cell types (Travis, 1965).

The cuticle is composed of four layers that vary in composition and thickness (Skinner, 1962, 1985; Travis, 1965). The thin outermost layer, the epicuticle, which is composed of protein, lipids, and calcium salts, has a dense bi-laminar organization. The two inner, thicker layers, the exocuticle and the endocuticle, comprise a calcified matrix composed of chitin–protein fibers stacked in layers of continuously changing orientation (Giraudguille, 1984; Roer and Dillaman, 1984). The innermost membranous layer contains chitin and proteins but lacks mineral deposits (Aiken and Waddy, 1987; Roer and Dillaman, 1984).

The crustacean molt cycle (Aiken and Waddy, 1987; Chang, 1995; Skinner, 1962, 1985) is divided into four stages, intermolt, premolt, ecdysis and postmolt. Intermolt is characterized by a fully developed cuticle and very low molt-related activity. Premolt is triggered by a surge of ecdysteroid molting hormones, which are converted in peripheral target tissues into the active hormone, 20-hydroxy ecdysone (20E). Premolt begins with partial digestion of the cuticular chitin and proteins and dissolution of the cuticular calcium (Shechter et al., 2008a; Wheatly and Ayers, 1995). In concert, new underlying exocuticle and epicuticle are secreted. At this stage, there is no major calcification in the new cuticle, which therefore remains flexible. During this time, the level of circulating ecdysteroids peaks and then falls to a low level close to ecdysis. Proliferation of the epithelial cells of the hypodermis occurs during premolt and return to the intermolt appearance after ecdysis (Johnson, 1980; Travis, 1965).

In certain crustacean species, some of the calcium that will be required later at postmolt for the formation of the new cuticle is reabsorbed from the old cuticle during premolt and stored in transient

Abbreviations: ACC, amorphous calcium carbonate; Cq-CDA1, *C. quadricarinatus* chitin deacetylase 1; GAP, gastrolith protein; GB, GenBank.

* Corresponding author. Tel.: +972 4 8565 257; fax: +972 4 8511 911.
E-mail addresses: yana@ocean.org.il (Y. Yudkovski), lilahg@bgu.ac.il (L. Glazer), rr@molgen.mpg.de (R. Reinhardt), veredcc@bgu.ac.il (V. Chalifa-Caspi), sagia@bgu.ac.il (A. Sagi), tom@ocean.org.il (M. Tom).

[1] Equally contributed the major part of the study.

1744-117X/$ – see front matter © 2010 Elsevier Inc. All rights reserved.
doi:10.1016/j.cbd.2010.03.010

calcium deposits (Travis, 1960; Ueno, 1980). In crayfish, including our model organism, the freshwater red claw crayfish *Cherax quadricarinatus*, these deposits comprise a pair of button-like structures, the gastroliths, which are formed in a cavity between a specialized hypodermis, the gastrolith disk, and the cuticular layer of the cardiac stomach (Shechter et al., 2008a; Travis, 1960; Travis and Friberg, 1963). The gastrolith disk is involved mainly in gastrolith formation during premolt, and upon completion of gastrolith growth — just before ecdysis — it becomes hypertrophied and folded and secrets the new epicuticle of the gastrolith region. During ecdysis, the old cuticle and the gastroliths collapse into the stomach, where they are digested. At postmolt the gastrolith disk deposits the exocuticle and the endocuticle of the gastrolith region and gradually shrinks to a minimum size at intermolt (Travis, 1960; Ueno, 1980). The rapid re-mineralization of the cuticle during postmolt relies on the calcium digested from the gastroliths together with exogenous calcium absorbed from the diet and the surrounding water (Greenaway, 1985).

The main mineral present in the calcified layers of the cuticle is calcium carbonate (Greenaway, 1985; Luquet and Marin, 2004; Wheatly and Ayers, 1995). In most crustaceans, the mineral appears in two forms, the stable crystalline calcite (Luquet and Marin, 2004; Pratoomchat et al., 2002; Yano, 1975) and the more soluble amorphous calcium carbonate (ACC) (Addadi et al., 2003; Greenaway, 1985; Shechter et al., 2008a; Sugawara et al., 2006). Recent studies suggest that ACC is the major form of the mineral in most temporary calcium carbonate deposits, such as the gastroliths. It is believed that the stabilization of the otherwise unstable ACC is mediated by specialized polypeptides and possibly other macromolecules (Addadi et al., 2003; Shechter et al., 2008b). In *C. quadricarinatus*, ACC is the most abundant form of calcium carbonate both in the cuticle and in the gastrolith. The cycle of degradation and deposition of ACC in these two structures involves deposition of ACC in the gastroliths concurrently with partial degradation of the cuticle during premolt and fast dissolution of the gastroliths concurrent with deposition of ACC in the new cuticle during postmolt (Shechter et al., 2008a).

To date, four proteins that are involved in calcium deposition have been identified in crustaceans: the gastrolith matrix protein (GAMP), orchestin, and the gastrolith proteins GAP 65 and GAP 10. GAMP, which was isolated from the crayfish *Procambarus clarkii* (Ishii et al., 1996, 1998), is believed to be a chitin-binding protein (Tsutsui et al., 1999). Orchestin is a calcium-binding protein that was isolated from the terrestrial crustacean *Orchestia cavimana* (Raz et al., 2002; Testeniere et al., 2002). GAP 65 (Shechter et al., 2008b) and GAP 10 (Glazer et al., 2010) are the first proteins to be characterized out of a number of structural proteins extracted from the *C. quadricarinatus* gastrolith matrix. The negatively charged calcium-binding GAP 65 glycoprotein is the most abundant structural protein in the gastrolith. It was demonstrated to have a dual role, stabilizing both the ACC and the spatial structure of the chitin matrix. It contains a chitin-binding domain, probably permitting the formation of protein–chitin cross-linking (Shechter et al., 2008b). GAP 10 does not contain a chitin-binding domain, but its deficiency decreases calcium deposition rate and lengthening the duration of the molt cycle (Glazer et al., 2010).

In the framework of our continuous effort to uncover the genes participating in the molt-related calcium carbonate cycle, the aim of this study was to reveal multi-gene expression patterns in the gastrolith disk and the hypodermis of *C. quadricarinatus* during late premolt by using a cDNA microarray platform.

2. Materials and methods

2.1. cDNA microarray

The cDNA microarray used here was similar to that previously used by our group (Yudkovski et al., 2007), which contained 4800 printed DNA fragments. Using the previously applied procedure, this microarray was broadened by the addition of 1000 cDNA fragments cloned from RNA preparations of premolt gastrolith disks (Glazer et al., 2010). Only relevant clones in the context of this study and the previous ones were sequenced. Sequences were annotated by using both BLASTX and BLASTN comparisons (Altschul et al., 1997). When available, gene ontology (GO) annotations (Ashburner et al., 2000) were borrowed from the BLAST hits, thereby further assisting the appropriate gene annotation. Both sequence and GO annotations were obtained with the BLAST2GO software (http://www.blast2go.de/; Conesa et al., 2005). Only BLAST hits with *e*-values $<10^{-5}$ and their derived GO terms were considered valid annotations.

2.2. Molt induction experiment

Before and during the experiment, *C. quadricarinatus* males were maintained in captivity at 28 °C with a photoperiod of 14L:10D0. The molt induction experiment was performed as described previously (Shechter et al., 2007). Briefly, intermolt male crayfish were divided into three groups. The animals of one group received multiple alpha-ecdysone injections and those of another group were subjected to the same protocol of sham-injections with the alpha-ecdysone carrier solution. The third group comprised intact, intermolt males. The molt stage was monitored by X-ray imaging of the gastrolith size, as described previously (Shechter et al., 2007). The alpha-ecdysone-injected crayfish were sacrificed at late premolt and the animals in the two intermolt groups were sacrificed at the same time. The characteristics and the molt indices of the treated and control crayfish are described in Table 1. Upon termination of the experiment, the gastrolith disk and the hypodermis of each animal were dissected out, immediately snap-frozen in liquid nitrogen and stored at −80 °C. In all the premolt individuals a new soft cuticle had already formed underneath the old one, and this cuticle and its underlying hypodermis were sampled from the carapace region. The intermolt hypodermis was removed from the inner side of the carapace. Total RNA and mRNA were purified from the frozen tissue, and their quality was tested as described by Yudkovski et al. (2007).

2.3. Design and analysis of the hybridized slides

The extracted mRNA populations from the hypodermis of the animals in the three groups were labeled and hybridized on

Table 1
Characteristics of *C. quadricarinatus* males used in the experiment. All animals were sacrificed 10 days after the beginning of the molt induction protocol. MMI — molt mineralization index (gastrolith width/carapace length; Shechter et al., 2007).

Tissue	Treatment group	No. of males	Average mass [g]	Average MMI [mm/mm]
Gastrolith disk	Ecdysone-injected — sacrificed at premolt	4	48 ± 5	0.084 ± 0.005
	Sham-injected — sacrificed (at intermolt) concurrently with the ecdysone-injected animals	4	65 ± 10	0
	Non-treated — sacrificed (at intermolt) concurrently with the ecdysone-injected animals	4	59 ± 15	0
Hypodermis	Ecdysone-injected — sacrificed at premolt	5	51 ± 10	0.083 ± 0.009
	Sham-injected — sacrificed (at intermolt) concurrently with the ecdysone-injected animals	5	67 ± 8	0
	Non-treated — sacrificed (at intermolt) concurrently with the ecdysone-injected animals	5	58 ± 13	0

microarray slides. The entire process of fluorescent labeling of the hybridized probes by Cy3 and Cy5 dyes, the hybridization procedure onto the microarray slides, and the slide imaging was carried out according to Yudkovski et al. (2007). Intermolt gastrolith disks revealed low RNA amounts. Hence they were linearly amplified by the indirect cDNA labeling method (TargetAmp 1-Round Amino-allyl-aRNA Amplification kit, Epicentre Biotechnologies, USA).

Individual variability was automatically integrated into the hybridization design (Fig. 1) by using the RNA populations of individual crayfish from each of the three groups, with the exception of the gastrolith disk of the sham-injected group, which was pooled into two samples before amplification due to low RNA levels. The hybridization design was based on independent biological replicates, each containing randomly selected individuals from each of the treatment groups. The design was balanced with respect to the dye labeling of the RNA populations, such that each individual RNA population was labeled with one dye in half of the biological replicates and with the other dye in the other half.

The calculation and statistical analysis of $\log_2$ expression ratios (M) and the $\log_2$ average signal intensity (mean A) for each clone across the experiment were carried out using the LIMMA package (Linear Models for Microarray Analysis; Smyth, 2005) according to Yudkovski et al. (2007), with the exception that the analytical procedure was modified to conform to the background characteristics and the distribution of the differentially expressed genes. Hence, extreme differentially expressed spots were specifically flagged manually on the Cy3–Cy5 scatter plot, created by the GenePix Pro 6.1, not to participate in the dual label normalization performed later by LIMMA. This elimination of extreme differentially expressed spots from the normalization procedure was necessary because of the dramatic elevation of gastrolith disk transcript levels at premolt. Only spots with a fluorescence intensity >500 arbitrary units (out of 65,536) in at least one of the dyes and which agreed with the GENEPIX Pro 6.1 eligibility criteria were used in the analysis. The Cy5 and Cy3 intensities within each slide were normalized by using the global LOWESS method, and background subtraction was applied. The inter-duplicate correlation method was used in the linear modeling step. Clones were considered differentially expressed within a binary comparison between experimental conditions when $p<0.01$, $M>2$ and mean $A>9$. The use of this stringent threshold was aimed at reducing false positive differential expressions.

2.4. Quantitative relative real-time PCR

The relative expression levels of target transcripts from the two compared *C. quadricarinatus* RNA populations were evaluated by using reverse transcription coupled with relative real-time PCR. The results were normalized to an entire gastrolith disk. Total RNAs were separately extracted from several late premolt or intermolt disks and were dissolved in equal volumes per disk. Identical aliquots were taken from each preparation and were reverse-transcribed at 42 °C for 1 h using suitable reverse primers, according to Sambrook and Russell (2001). PCR reactions, using as templates the reverse transcriptase solutions of each RNA population, were accomplished for selected target genes. Each reaction was performed in triplicates using a StepOne plus PCR device (Applied Biosystems) (1 cycle at 95 °C, 10 min; 40 cycles at 95 °C, 15 s and 60 °C, 1 min). Crossing point (CP) is the PCR cycle in which the fluorescent intensity crosses the threshold of detection, and the difference between the levels of each of the examined transcripts when comparing premolt and late premolt individuals was expressed in ΔCP values. A standard PCR reaction was composed of 5 μL SYBR Green mix (Applied biosystems), 1 μL of 2 pmol/μL of each of the PCR primers and 2 μL aliquot sample from the reverse transcription mixture, completed to a total volume of 10 μL by water.

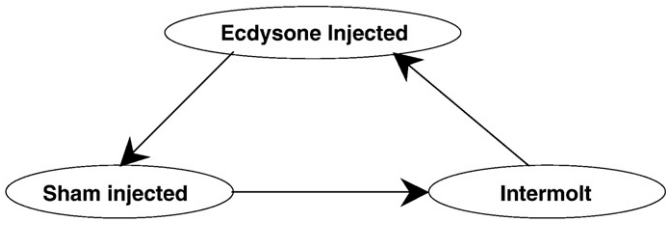

Fig. 1. Hybridization design. Ellipses designate single males from the three participating groups. Each arrow connects two RNA populations hybridized onto one slide: arrowhead — Cy3 labeling, tail — Cy5 labeling. Alternate arrow directions were used in different biological replicates to compensate for putative dye effects.

2.5. Sequencing of Cq-CDA1 transcript

5′- and 3′-rapid amplification of cDNA ends (RACE) were carried out using the FirstChoice® RLM-RACE kit (Ambion Inc, Austin, TX, USA) and the Clontech SMARTer™ RACE kit (Clontech Laboratories Inc., Mountain View, CA, USA), according to the manufacturers' protocols, to obtain the entire ORF sequence. The deduced amino acid sequence of the gene was obtained by the Expasy Translate tool (http://www.expasy.org/tools/dna.html), the putative signal peptide was predicted using SignalP 3.0 CBS Prediction Servers (http://www.cbs.dtu.dk/services), and the putative ChtBD2 and Polysaccharide deacetylase domains were predicted by SMART (http://smart.embl-heidelberg.de/).

3. Results

3.1. Differentially expressed genes

Only one clone revealed differential expression between intact intermolt and sham-injected individuals in both examined organs. It was the down-regulated non-annotated GB ID: DQ847664.

Differentially expressed genes in the *C. quadricarinatus* hypodermis and gastrolith disk are listed in Tables 2 and 3. Each unique clone is characterized by the M index, determining the intensity and direction of its differential expression in comparison to sham-injected intermolt individuals. GenBank accession number and when available annotated function, were assigned to each clone. The differential expression at premolt in the gastrolith disk is almost entirely characterized by up-regulation. Among the up-regulated genes are three structural proteins of the crustacean cuticle and gastrolith: GAP 10 (Glazer et al., 2010), apocrustacyanin C2A chain A, which is part of

Table 2
Annotated and non-annotated, differentially expressed genes in the *C. quadricarinatus* hypodermis. Alpha-ecdysone-injected vs. sham-injected males. Grey-highlighted clones were mutually differentially expressed in the hypodermis and the gastrolith disk. All accession numbers in the table were deposited in GenBank.

GB accession number	*M* value	Annotation
Various		
DQ847750	−3.07	Similarity to crustacean anti-lipopolysaccharide factor
DQ847679	−2.25	Astacidin 2 antimicrobial peptide
GQ286151	−3.89	Conserved hypothetical protein (*Culex quinquefasciatus*)
Gastrolith structural proteins		
FJ361143	−2.54	GAP 10 (acc. no. of the full length cDNA: GQ231313)

GB accession number	*M* value	GB accession number	*M* value	GB accession number	*M* value
Non-annotated genes					
DQ847548	−4.65	DQ847759	−4.00	EF692595	−5.93
DQ847664	−3.59	DQ847778	−3.00	FJ361173	−4.41
DQ847568	−3.83	DQ847903	−3.06	GQ286171	−2.57
		EF692588	−3.06		

Table 3
Annotated and non-annotated, differentially expressed genes in the *C. quadricarinatus* gastrolith disk. Alpha-ecdysone-injected vs. sham-injected males. Grey-highlighted clones were mutually differentially expressed in the hypodermis and the gastrolith disk. All accession numbers in the table were deposited in GenBank.

GB accession number	*M* value	Annotation
Non-annotated insect genes		
FJ361175	2.06	Similar to several non-annotated insect proteins
GQ286150	4.01	Similar to several non-annotated insect proteins
EF692605	2.56	Similar to several non-annotated insect proteins
FJ361131	2.19	Similar to several non-annotated insect proteins
FJ361129	4.59	Similar to several non-annotated insect proteins
DQ847540	3.85	Similar to several non-annotated insect proteins
Putative signal transduction-related gene		
GQ286096	3.16	Insect DNA-binding nuclear protein p8
Translation-related genes		
GQ286088	3.07	Ribosomal protein S3
FJ361136	2.28	Ribosomal protein S20 40S
FJ361179	2.87	Ribosomal protein S20 40S
FJ361138	2.13	Ribosomal protein S30e
GQ286156	2.09	Ribosomal protein L15
FJ361125	2.39	Ribosomal protein 27a
DQ847534	2.10	Elongation factor 1-alpha
Energy provision-related genes		
DQ847786	2.34	NADH-ubiquinone oxidoreductase chain 4 - crustacean
DQ847742	4.51	NADH dehydrogenase subunit 1
FJ361139	3.25	Zinc finger protein; cytochrome C oxidase polypeptide VIIc
GQ286102	3.90	ATP synthase subunit g - H transporting
DQ847537	2.13	Cytochrome C oxidase subunit I
FJ361141	3.78	ATP synthase E chain
FJ361133	2.87	Arginine kinase - crustacean
Cellular structural genes		
DQ847930	3.35	Alpha-I tubulin - crustacean
GQ286146	2.70	Alpha-I tubulin - crustacean
DQ847595	−2.04	Actin - crustacean
DQ847570	3.43	Beta actin - crustacean
Extracellular structural genes		
FJ361143	3.98	GAP 10 (acc. No. of the full length cDNA:)
DQ847765	4.06	Cq-CDA1 (acc. No. of the full length cDNA: GQ421322)
DQ847718	2.23	Apocrustacyanin C2A chain A - crustacean
Various		
DQ847679	3.04	Astacidin 2 antimicrobial peptide

GB accession number	*M* value	GB accession number	*M* value	GB accession number	*M* value
Non-annotated genes					
DQ847543	3.19	DQ847903	3.89	GQ286087	3.09
DQ847546	3.54	DQ847906	2.57	GQ286106	3.68
DQ847568	3.47	DQ847921	3.70	GQ286152	−5.07
DQ847647	4.50	DQ847922	2.53	GQ286153	2.6
DQ847648	2.25	DQ847988	3.26	GQ286159	2.95
DQ847660	3.07	FJ361119	2.59	GQ286160	2.48
DQ847708	2.13	FJ361127	2.94	GQ286161	5.7
DQ847727	3.93	FJ361130	2.09	GQ286162	3.73
DQ847737	2.42	FJ361140	4.44	GQ286163	4.13
DQ847752	2.27	FJ361144	4.48	GQ286164	4.22
DQ847790	3.53	FJ361161	−3.15	GQ286165	5.31
DQ847826	3.06	FJ361173	3.65	GQ286167	4.52
DQ847837	2.22	FJ361174	2.45	GQ286170	2.64
		GQ286086	3.05	GQ286171	3.21

a pigment–protein cuticular complex (Zagalsky et al., 1991), and a protein, designated by us as Cq-chitin deacetylase1 (Cq-CDA1), which resembles one of the vermiform-like cuticular proteins (Ver1) of the crab *Portunus pelagicus* (Kuballa et al., 2007) and members of the large insect chitin deacetylase gene family (Dixit et al., 2008).

A full length cDNA sequence of the Cq-CDA1 was elucidated using RACE-PCR and was deposited in GenBank under the accession number GQ421322, including its deduced protein sequence and the identified domains. The deduced protein contains 489 amino acids (AAs), its molecular weight is 55,518 Da and its theoretical pI is 4.59. Three domains were identified in the protein sequence, a putative signal peptide between AAs 1 and 20, a putative chitin-binding domain 2 (ChtBD2) between AAs 23 and 77 and a putative chitin deacetylase domain (CDA) between AAs 123 and 256. Two putative N-glycosylation sites were identified between AAs 153–155 and 434–436, respectively. ChtBD2 was significantly identified using domain-finding software. In contrary, the similarity of the Cq-CDA1 CDA domain to a consensus polysaccharide deacetylase sequence was not significant. Cq-CDA1 protein sequence resembles that of members of the large insect chitin deacetylase gene family (Dixit et al., 2008). Hence, the boundaries of its chitin deacetylase domain were determined by comparisons to the corresponding insect sequences. Sequence comparisons of the two domains among several crustacean and insect CDAs are presented in Fig. 2. The consensus of the polysaccharide deacetylase family, including Cq-CDA1 contains several conserved cysteines throughout the open reading frame sequence.

Intensive cell proliferation, metabolic activity, and protein synthesis activities are indicated by the other prominently up-regulated groups. The up-regulated cytoskeletal proteins beta-actin and alpha I tubulin and the up-regulated DNA-binding nuclear protein P8, a transcription co-factor (Qiu and MacRae, 2007), are indicative of cell proliferation. Intensive translation is indicated by up-regulated ribosomal proteins and elongation factor-1 alpha. Genes related to ATP synthesis are indicative of high energy requirements of the gastrolith construction process. No annotation or only general insect-related origin was assigned to approximately half of the differentially expressed genes. The differentially expressed hypodermal genes, including GAP 10, were mainly down-regulated during the late premolt stage.

The cDNA microarray platform and the dataset of the gastrolith disk and hypodermal hybridizations were deposited in the Gene Expression Omnibus (GEO) database of the American National Center for Biotechnology Information (NCBI). The platform was assigned GEO accession number — GPL8761, and the gastrolith disk and hypodermal dataset assigned the accession number GSE16866. (http://www.ncbi.nlm.nih.gov/geo/query/acc.cgi?token=xhkzjaqmmewugrk&acc=GSE16866).

3.2. Quantitative PCR validation of microarray results

The microarray results were validated by binary comparisons of the relative expression levels of selected unique clones by quantitative relative real-time PCR (RT-qPCR). Selected RNA populations of native and ecdysone-injected tissue were used. The selected RNA pairs of late premolt and intermolt individuals were also mutually hybridized on one microarray slide. The results, normalized to an entire gastrolith disk, are presented in Table 4, where they are compared to the respective microarray *M* values. Much larger differences in gene expression levels between intermolt and premolt disks were revealed by the real-time PCR compared to the corresponding *M* values, originating from the hybridizations. In addition, a 1000-fold increase in ribosomal RNA production/disk was revealed. The difference between the microarray and the real-time PCR results is discussed below, in relation to the appropriate normalization of gene expression levels in the dramatically activated gastrolith disk during the intermolt–premolt transition.

4. Discussion

A multi-gene approach aimed at identifying genes involved in late premolt-related processes in the crustacean hypodermis and gastrolith disk was used here for the first time. The gastrolith disk undergoes a dramatic change of activity during the transition from intermolt to

Chitin binding domain 2

```
Cq - FTCPE--PEGQFASDQNCKVFYQCVGGFPYRQRCAEGSYYDGSKHECVSRFDPNIKCGP
Ap - FVCPEVGGNGNYADPATCRRFYQCVDNFPYLNRCPAGLYFDDVNKLCT--FKNEARCGP
Tc - FECPQGVGNGNFADPATCRRFYQCVDGYPYLNRCPSGLFFDDISKFCT--FKNEARCGP
Cqu- FKCPEGYGNGNFADPATCRRFYQCVDGYPYVNRCPSGLYFDDVQKFCT--FKAEAKCGP
Am - FKCPEGQGNGNFADPATCRRFYQCVDGYPYLNRCPSGLHFDDISKFCT--FKNEARCGP
-------------------------------------------------------------
Con- F CP+--  G +A    C+ FYQCV  +PY  RC  G ++D     C --F    +CGP
```

Chitin deacetylase domain

```
Cq - VEVPQMIMLTFDGAINDLNFETYSKIFLDNRTNPNGCPIRGTFFVSHEYTNQLVEKFYSR
Ap - KETPQMILLTFDGALNQNNYDHYQKVFSHNKKNPNGCLIKGTFFISHEYCDNMVQEIAHK
Tc - EETPQMILMTFDGAINLNNYDHYKKVFNKKRQNPNGCDIRGTFFISHEYSNQMIQGLASD
Cqu- DEIPQIILLTFDGAVNLNNYEHYKKVFNGKRQNPNGCDIKGTFFISHEYSNQQIQVLANG
Am - DETPQMIIMTFDGAINHNNFDHYQKIFATDRLNPNNCPLKGTFFISHEYCNNMVQSLAHD
Pp -        MLTVDGAVNDLNYETYSSVFRPDRTNPNGCPIRGTFFVSHEYTNQQGEDLYSR
-------------------------------------------------------------
Con-  E PQ+I++T DGA+N  N++ Y  +F   + NPN CP++GTFF+SHEY +   +

Cq - GHEIAVGTVSRRAGLEDEGEETWIGETVTMKEILQRFAGVRPDIKGVRGPHLKPGRDAQY
Ap - GHEIAVETVSLQKGLHDKGYEEWVAEMIGMREILVNFANLTKDIVGMRAPFLKPGRNTQY
Tc - GHEMATETISLQMGLQDKGYEEWVGEMIGMREILRHFANISKQVVGMRAPFLKPGRNTQY
Cqu- GHEIAVETISLQQGLQDKGYEEWVGEMIGMRSILKHFSNVSSEINGMRAPFLKPGRNQYK
Am - GHEIATETISLQKGLEDKGYEEWVGEMIGMREILKHFSNISIEIVGMRAPYLKPGRNQYK
Pp - GHEIAVGSVSRRAGLEDEGEESWTGEMVTMREILTKFAGVRTDLKGQRGPHLKPGREAQY
-------------------------------------------------------------
Con- GHEIA  ++S + GL D+G E W+ E + M+ IL  F+ +   + G R P LKPGR+ QY

Cq - EVLSAYDFTWD
Ap - EVIEDYGFVYD
Tc - KVLEDFGYIYD
Cqu- KVIEDFGFIYD
Am - KVVEDFGYIYD
Pp - EVLSAYGFTWD
----------------
Con- +V+  + + +D
```

Fig. 2. Similarities of the chitin-binding domain 2 and the chitin deacetylase domain among arthropod species. Cq — *C. quadricarinatus* chitin deacetylase 1 — GB ID: GQ421322, Ap — *Acyrthosiphon pisum* — GB ID: XP_001951879, Tc — *Tribolium castaneum* — GB ID: NP_001103903, Cqu — *Culex quinquefasciatus* — GB ID: XP_001848017, Am — *Apis mellifera* — GB ID: XP_001120478, Pp — *Portunus pelagicus* — GB ID: ABM54470, con — consensus bases across the presented sequences. (+) Designates replacement of one base in the AA codon, (−) designates gap.

premolt. Both cell size and number increase (Travis, 1960), and the amount of RNA extracted per disk, demonstrated by the 16S rRNA level/disk, is roughly 1000-fold higher in the late premolt stage than in the intermolt stage (Table 4). Ribosomal RNA in general, is economically produced to meet the cellular requirements, which are here mainly growth, proliferation and protein secretion, via several partially known regulatory pathways (Mayer and Grummt, 2006; Warner, 1999). Thus, the requirements of the resting intermolt gastrolith disk differ markedly from those of the growing and proliferating premolt one, producing proteins both for its maintenance and for secretion into the gastrolith cavity to participate in the gastrolith formation. The method applied here for the normalization of the microarray results made use of all transcripts that were equally labeled at the two compared molt cycle stages. However, the RNA used for the labeling of the intermolt gastrolith disk was amplified to compensate for the absolute low expression levels and to meet the required amounts needed for the labeling. Hence, equally labeled spots comparing intermolt to premolt, represent all genes for which the level of expression/disk increased roughly by the same factor at the intermolt–premolt transition. Consequently, the apparent up-regulation represents expression levels exceeding this general huge increase in expression. In contrast, the apparent down-regulation, revealed in three clones, FJ361161, GQ286152 and DQ847595 represent assumedly attenuated up-regulation and not an actual reduction in premolt expression levels vis-à-vis intermolt levels.

Comparison by RT-qPCR of transcript expression levels in a given tissue for two different biological situations is relatively easy when the energy consumption of the tissue, the overall transcription level, or the cellular growth and proliferation are relatively constant. In such a case, rRNA-related parameters as well as cytoskeletal, metabolic or translation-related genes may serve as normalizing agents (e.g., Radonić et al., 2004; Pérez et al., 2008). However, it is clearly demonstrated in Table 3 that the expression of cytoskeletal elements, genes related to energy provision, translation-related genes during the intermolt - premolt transition exceeds the general increase of transcription activity, rendering them not adequate for normalization of RT-qPCR results. Table 4 demonstrated also similar increase of rRNA production. Consequently, an entire disk was used here as the normalizing unit for the RT-qPCR validation of the microarray results. Both M values and ΔCPs represent $\log_2$ fold-expression between the compared RNA populations, and although evaluated by different methods, they can be qualitatively compared. The marked difference between these two parameters for each evaluated expression (Table 4) is probably due to the general increase in the activity of the tissue in the premolt stage. It has to be emphasized that the increased size of the gastrolith disk is unusually extreme. The 1000-fold increase in rRNA levels per disk may be an overestimation caused by higher efficiency of RNA extraction from the bigger premolt organ, however, several hundred-fold increase is considered reasonable estimate.

The gene expression patterns in the two target hypodermal tissues demonstrated opposite tendencies during the late premolt stage, within the limits of the present cDNA assemblage. The functions of both tissue types include the formation of mineral–chitin–protein

Table 4
Differential expression of selected genes between intermolt and late premolt *C. quadricarinatus* individuals. Differential expression was evaluated by real-time PCR and normalized to a single gastrolith disk. Crossing point (CP) is the PCR cycle in which the fluorescent intensity crosses the threshold of detection, and the difference between the levels of each of the examined transcripts when comparing premolt and late premolt individuals was expressed in ΔCP values. The difference in PCR cycles (ΔCP) between the two time points of the molt cycle (intermolt and late premolt) was compared to the *M* values obtained from the microarray hybridization analysis. All accession numbers in the table were deposited in GenBank.

GB accession number	Gene description	PCR primer pair	ΔCP	*M* value
GQ286150	Similar to several non-annotated insect proteins	F: GGC AAG AGC AAT AAC AAC CCC R: TGT CAG ACT TGC CAG TTC CCC	16.3	4.01
GQ286096	Insect DNA-binding nuclear protein P8	F: GCT CTC ACC ATG TCG GAT GC R: TGC TTG GAG CGG TTC TTT CC	7.2	3.15
DQ847930	Alpha-I tubulin	F: TAG TCC CTG GTG GAG ATT TGG C R: AAA TTT GTG ATC CAG ACG TGC C	11.1	3.35
GQ286086	No annotation	F: GGA GCT TAA CAA GAG AGC CGA CTG R: CTG GTT GGT TTT CAT TTT AGG TGC	8.3	3.05
FJ361131	Similar to several non-annotated insect proteins	F: CGT CAG TGC AAG GCT CAA CAC R: GAG GCC ACA AGT TGC TGC TG	6.1	2.19
DQ847718	Apocrustacyanin C2A chain A	F: CGC TTC ACG AAC TTG TCT GCC R: TCG CCT GCA TAT ACT CCT GCC	7.2	2.23
DQ847570	Beta actin	F: TCT CGT TCA GCA GTG GTA GCG R: GCT ATC TTG CGT CTC GAC TTG G	–[a]	3.13
DQ847728	16S RNA	F: CCT TCG CAC GGT CAA AAT ACC R: AGT CTG ACC TGC CCA TTG GG	10	

[a] No PCR product in the intermolt gastrolith disk disabling the calculation of a ΔCP value.

complexes. For the hypodermis, this process — the construction of the cuticle — takes place gradually over the entire premolt and postmolt period. It comprises dissolution of the inner cuticular layers, deposition of the new epicuticle and the exocuticle during premolt, and deposition of the endocuticle and the membranous layer, accompanied by cuticular calcification, during postmolt (Travis, 1965). The gastrolith disk, in contrast, demonstrates a biphasic process of construction of two mineral–chitin–protein complexes, i.e., deposition of the gastrolith during the greater part of the premolt stage, followed by the construction of the new cuticle during the very late premolt and postmolt stages. The proliferation of the epithelium of the gastrolith disk after deposition of the gastrolith but before ecdysis (Ueno, 1980) is probably related to the synthetic activity of the new cuticle. The overwhelming and pronounced up-regulation of energy-provision related genes, translation-related genes and structural proteins in the gastrolith disk during the late premolt stage may be attributed both to gastrolith deposition and to the preparatory epithelial proliferation preceding cuticular deposition. The up-regulation of cytoskeletal proteins is probably due to the late premolt epithelial proliferation.

Two proteins, GAP 65 (Shechter et al., 2008b) and GAP 10 (Glazer et al., 2010), were extracted by us from the gastrolith and then characterized. Even though there were strong indications that these proteins are components of the gastrolith structure, there were also indications that their transcripts are expressed in both the gastrolith disk and the hypodermis. Although levels of both GAP 65 and GAP 10 proteins were high in the gastrolith matrix, the two genes elicited different relative transcription levels at late premolt. GAP 65 exhibited minor transcription activity in contrast to the high activity of GAP 10. This difference may be explained by the different functions of the two proteins and indicates possible prolonged production of the GAP 10 protein, which may also be required for the construction of the new gastrolith-enveloping cuticle.

Prior to the present study, crustacyanin had been identified only in the crustacean cuticle. Crustacyanin functions in pigment binding (Zagalsky et al., 1991) and its role in the pigmentless gastrolith disk is not known. Cq-CDA1 is similar to a rather large family of insect and crustacean extracellular chitin deacetylase (CDA)-like proteins. These proteins contain in arthropods up to three domains, the chitin-binding domain 2 (ChtBD2), the LDLa and the CDA domains (Dixit et al., 2008). The extracellular GAP 65 (GB ID: EU551670) contains all three domains, and was demonstrated to be involved in the spatial structure of the chitin matrix (Shechter et al., 2008b). Cq-CDA1 lacks the LDLa domain, but contains both the ChtBD2 and the CDA domains. This pattern may suggest that Cq-CDA1 retains its chitin-binding activity. The CDA catalytic domain is probably inactive, similar to other CDA-like proteins from this family (Dixit et al., 2008). However, the appropriate placement of several highly conserved amino acids along the CDA domain across arthropods indicates a yet to be discovered function. The presence of signal peptide in GAP 10, GAP 65 and Cq-CDA1 as well as the presence of the two former proteins in the gastrolith organic matrix indicate their secretion to the extracellular space. Last but not least, the general resemblance of Cq-CDA1 to other members of the polysaccharide deacetylase members and the presence of several conserved cysteines throughout the protein sequence indicates similar three dimensional protein structure, hence, mutual function.

The marked down-regulation of the hypodermis in the late premolt stage is an unexpected finding, since the hypodermis was described as active during that stage and the growth of the hypodermal epithelium peaks during late premolt (Johnson, 1980; Travis, 1965). A postulated inactive period between probable two more active ones at the preceding early premolt and the following postmolt, may explain the down-regulation in the late premolt stage. We observed that the new cuticle was already present at late premolt, the termination time point of the experiment, while the remainder of its construction — deposition of the endocuticle and the membranous layer and calcification — is postponed to postmolt (Shechter et al., 2008a). Hence an expression low may be hypothesized. Five differentially expressed genes (Tables 2 and 3) were differentially expressed in both tissues, albeit with opposite expression levels.

It is evident that a hybridization experiment that covers the entire premolt–postmolt period is required to elucidate the complete pattern of gene expression in the two related tissues, the hypodermis and the gastrolith disk. In addition, utilization of state-of-the-art sequencing and microarray techniques may broaden the number of screened transcripts and increase sensitivity of the array.

Acknowledgements

The study was supported by the Israel Science Foundation grant No. 1080/05. We thank Dr. Miriam Kott-Gutkowski of the Faculty of Medicine, The Hebrew University of Jerusalem for provision of microarray-related services. We wish to thank Mr. Liron Friedman for keeping the animals, Mr. Rotem Kadir is appreciated for his assistance in sequencing the Cq-CDA1, and Ms. Inez Mureinik is thanked for the English editing.

References

Addadi, L., Raz, S., Weiner, S., 2003. Taking advantage of disorder, amorphous calcium carbonate and its roles in biomineralization. Adv. Mater. 15, 959–970.

Aiken, D.E., Waddy, S.L., 1987. Molting and growth in crayfish, a review. Can. Tech. Rep. Fish. Aquat. Sci. 1587, 1–34.

Altschul, S.F., Madden, T.L., Schäffer, A.A., Zhang, J., Zhang, Z., Miller, W., Lipman, D.J., 1997. Gapped BLAST and PSI-BLAST, a new generation of protein database search programs. Nucleic Acids Res. 25, 3389–3402.

Ashburner, M., Ball, C.A., Blake, J.A., Botstein, D., Butler, H., Cherry, J.M., Davis, A.P., Dolinski, K., Dwight, S.S., Eppig, J.T., Harris, M.A., Hill, D.P., Issel-Tarver, L., Kasarskis, A., Lewis, S., Matese, J.C., Richardson, J.E., Ringwald, M., Rubin, G.M., Sherlock, G.C., The Gene Ontology Consortium, 2000. Gene ontology, tool for the unification of biology. Nat. Genet. 25, 25–29.

Chang, E.S., 1995. Physiological and biochemical changes during the molt cycle in decapod crustaceans, an overview. J. Exp. Mar. Biol. Ecol. 193, 1–14.

Conesa, A., Gotz, S., Garcia-Gomez, J.M., Terol, J., Talon, M., Robles, M., 2005. Blast2GO, a universal tool for annotation, visualization and analysis in functional genomics research. Bioinformatics 21, 3674–3676.

Dixit, R., Arakane, Y., Specht, C.A., Richard, C., Kramer, K.J., Beeman, R.W., Muthukrishnan, S., 2008. Domain organization and phylogenetic analysis of proteins from the chitin deacetylase gene family of *Tribolium castaneum* and three other species of insects. Insect Biochem. Mol. Biol. 38, 440–451.

Giraudguille, M.M., 1984. Fine structure of the chitin protein system in the crab cuticle. Tissue Cell 16, 75–92.

Glazer, L., Shechter, A., Tom, M., Yudkovsky, Y., Weil, S., Aflalo, E.D., Pamuru, R.R., Berman, A., Bentov, S., Sagi, A., 2010. A protein involved in the assembly of an extracellular calcium storage matrix. J. Biol. Chem. 285, 12831–12839.

Greenaway, P., 1985. Calcium balance and molting in the Crustacea. Biol. Rev. Cambridge Philos. Soc. 60, 425–454.

Ishii, K., Yanagisawa, T., Nagasawa, H., 1996. Characterization of a matrix protein in the gastroliths of the crayfish *Procambarus clarkii*. Biosci. Biotechnol. Biochem. 60, 1479–1482.

Ishii, K., Tsutsui, N., Watanabe, T., Yanagisawa, T., Nagasawa, H., 1998. Solubilization and chemical characterization of an insoluble matrix protein in the gastroliths of a crayfish, *Procambarus clarkii*. Biosci. Biotechnol. Biochem. 62, 291–296.

Johnson, P.T., 1980. Histology of the Blue Crab, *Callinectes sapidus*. A Model for the Decapoda. Praeger Publications, N.Y.. 440 pp.

Kuballa, A.V., Merritt, D.J., Elizur, A., 2007. Gene expression profiling of cuticular proteins across the moult cycle of the crab *Portunus pelagicus*. BMC Biol. 5, 45.

Luquet, G., Marin, F., 2004. Biomineralisations in crustaceans, storage strategies. C.R. Palevol. 3, 515–534.

Mayer, C., Grummt, I., 2006. Ribosome biogenesis and cell growth, mTOR coordinates transcription by all three classes of nuclear RNA polymerases. Oncogene 25, 634–639.

Pérez, R., Tupac-Yupanqui, I., Dunner, S., 2008. Evaluation of suitable reference genes for gene expression studies in bovine muscular tissue. BMC Mol. Biol. 9, 79.

Pratoomchat, B., Sawangwong, P., Guedes, R., Reis, M.D., Machado, J., 2002. Cuticle ultrastructure changes in the crab *Scylla serrata* over the molt cycle. J. Exp. Zool. 293, 414–426.

Qiu, Z., MacRae, T.H., 2007. Developmentally regulated synthesis of p8, a stress-associated transcription cofactor, in diapause-destined embryos of *Artemia franciscana*. Cell Stress Chaperones 12, 255–264.

Radonić, A., Thulke, S., Mackay, I.M., Landt, O., Siegert, W., Nitschea, A., 2004. Guideline to reference gene selection for quantitative real-time PCR. Biochem. Biophys. Res. Commun. 313, 856–862.

Raz, S., Testeniere, O., Hecker, A., Weiner, S., Luquet, G., 2002. Stable amorphous calcium carbonate is the main component of the calcium storage structures of the crustacean *Orchestia cavimana*. Biol. Bull. 203, 269–274.

Roer, R., Dillaman, R., 1984. The structure and calcification of the crustacean cuticle. Am. Zool. 24, 893–909.

Sambrook, J., Russell, D.W., 2001. Molecular Cloning, a Laboratory Manual, Third edition. Cold Spring Harbor Laboratory Press, Cold Spring Harbor, NY.

Shechter, A., Tom, M., Yudkovski, Y., Weil, S., Chang, S.A., Chang, E.S., Chalifa-Caspi, V., Berman, A., Sagi, A., 2007. Search for hepatopancreatic ecdysteroid-responsive genes during the crayfish molt cycle, from a single gene to multigenicity. J. Exp. Biol. 210, 3525–3537.

Shechter, A., Berman, A., Singer, A., Freiman, A., Grinstein, M., Erez, J., Aflalo, E.D., Sagi, A., 2008a. Reciprocal changes in calcification of the gastrolith and cuticle during the molt cycle of the red claw crayfish *Cherax quadricarinatus*. Biol. Bull. 214, 122–134.

Shechter, A., Glazer, L., Cheled, S., Mor, E., Weil, S., Berman, A., Bentov, S., Aflalo, A.D., Khalaila, I., Sagi, A., 2008b. A gastrolith protein serving a dual role in the formation of an amorphous mineral containing extracellular matrix. Proc. Natl. Acad. Sci. U. S. A. 105, 7129–7134.

Skinner, D.M., 1962. The structure and metabolism of a crustacean integumentary tissue during a molt cycle. Biol. Bull. 123, 635–647.

Skinner, D.M., 1985. Molting and regeneration. In: Bliss, D.E., Mantel, L.H. (Eds.), The Biology of Crustacea, vol. 9. Academic Press, New York, pp. 43–146.

Smyth, G.K., 2005. LIMMA: linear models for microarray data. In: Gentleman, R., Carey, V.J., Huber, W., Irizarry, R.A., Dudoit, S. (Eds.), Bioinformatics and Computational Biology Solutions Using R and Bioconductor, Statistics for Biology and Health. Springer, New York, NY, pp. 397–420.

Sugawara, A., Nishimura, T., Yamamoto, Y., Inoue, H., Nagasawa, H., Kato, T., 2006. Self-organization of oriented calcium carbonate polymer composites, effects of a matrix peptide isolated from the exoskeleton of a crayfish. Angew. Chem. Int. Ed. Engl. 45, 2876–2879.

Testeniere, O., Hecker, A., Le Gurun, S., Quennedey, B., Graf, F., Luquet, G., 2002. Characterization and spatiotemporal expression of orchestin, a gene encoding an ecdysone-inducible protein from a crustacean organic matrix. Biochem. J. Rev. 361 (Pt 2), 327–335.

Travis, D.F., 1960. The deposition of skeletal structures in the Crustacea. 1. The histology of the gastrolith skeletal tissue complex and the gastrolith in the crayfish, *Orconectes* (cambaus) *verilis* Hagen - Decapoda. Biol. Bull. 16, 137–149.

Travis, D.F., 1965. The deposition of skeletal structures in the crustacea. 5. The histomorphological and histochemical changes associated with the development and calcification of the branchial exoskeleton in the crayfish *Orconectes virilis* Hagen. Acta Histochem. 20, 193–222.

Travis, D.F., Friberg, U., 1963. The deposition of skeletal structures in the crustacea. IV. Microradiographic studies of the gastrolith of the crayfish *Orconectes virilis* Hagen. J. Ultrastruct. Res. 8, 48–65.

Tsutsui, N., Ishii, K., Takagi, Y., Watanabe, T., Nagasawa, H., 1999. Cloning and expression of a cDNA encoding an insoluble matrix protein in the gastroliths of a crayfish, *Procambarus clarkii*. Zool. Sci. (Tokyo) 16, 619–628.

Ueno, M., 1980. Calcium-transport in crayfish gastrolith disk — morphology of gastrolith disk and ultrahistochemical demonstration of calcium. J. Exp. Zool. 213, 161–171.

Warner, J.R., 1999. The economics of ribosome biosynthesis in yeast. Trends Biochem. Sci. 24, 437–440.

Wheatly, M.G., Ayers, J., 1995. Scaling of calcium, inorganic contents, and organic contents to body-mass during the molting cycle of the fresh-water crayfish *Procambarus clarkii* (Girard). J. Crust. Biol. 15, 409–417.

Yano, I., 1975. An electron microscope study on the calcification of the exoskeleton in the shore crab. Bull. Jap. Soc. Fish. Oceanogr. 41, 1079–1082.

Yudkovski, Y., Shechter, A., Chalifa-Caspi, V., Auslander, M., Ophir, R., Dauphin-Villemant, C., Waterman, M., Sagi, A., Tom, M., 2007. Hepatopancreatic multi-transcript expression patterns in the crayfish *Cherax quadricarinatus* during the moult cycle. Insect Mol. Biol. 16, 661–674.

Zagalsky, P.F., Eliopoulos, E.E., Findlay, J.B.C., 1991. The lobster carapace carotenoprotein, alpha-crustacyanin, a possible role for tryptophan in the bathochromic spectral shift of protein-bound astaxanthin. Biochem. J. 27, 79–83.